

1 Wet-season spatial variability of N₂O emissions from a tea field in subtropical central China

2

3 X. Fu^{1,*}, X. Liu^{1,*}, Y. Li¹, J. Shen¹, Y. Wang¹, G. Zou¹, H. Li¹, L. Song¹, and J. Wu¹

4

5 ¹Changsha Research Station for Agricultural & Environmental Monitoring and

6 Key Laboratory of Agro-ecological Processes in Subtropical Regions,

7 Institute of Subtropical Agriculture, Chinese Academy of Sciences,

8 Hunan 410125, China

9 *These two authors contributed equally to this work.

10 Correspondence to: Professor Yong Li

11 Institute of Subtropical Agriculture,

12 Chinese Academy of Sciences, Hunan 410125, China

13 Tel: +86-731-8461-5291

14 Fax: +86-731-8461-2685

15 E-mail: yli@isa.ac.cn

16

17 **Abstract**

18 Tea fields emit large amounts of nitrous oxide (N₂O) to the atmosphere. Obtaining accurate
19 estimations of N₂O emissions from tea-planted soils is challenging due to strong spatial
20 variability. We examined the spatial variability of N₂O emissions from a red-soil tea field in
21 Hunan province, China, on 22 April 2012 (in a wet season) using 147 static mini chambers
22 approximately regular gridded in a 4.0 ha tea field. The N₂O fluxes for a 30-min snapshot
23 (10–10.30 a.m.) ranged from –1.73 to 1659.11 g N ha⁻¹ d⁻¹ and were positively skewed with
24 an average flux of 102.24 g N ha⁻¹ d⁻¹. The N₂O flux data were transformed to a normal
25 distribution by using a logit function. The geostatistical analyses of our data indicated that the
26 logit-transformed N₂O fluxes (FLUX30t) exhibited strong spatial autocorrelation, which was
27 characterized by an exponential semivariogram model with an effective range of 25.2 m. As
28 observed in the wet season, the logit-transformed soil ammonium-N (NH₄Nt), soil nitrate-N
29 (NO₃Nt), soil organic carbon (SOct), total soil nitrogen (TSNt) were all found to be
30 significantly correlated with FLUX30t ($r = 0.57-0.71$, $p < 0.001$). Three spatial interpolation
31 methods (ordinary kriging, regression kriging and cokriging) were applied to estimate the
32 spatial distribution of N₂O emissions over the study area. Cokriging with NH₄Nt and NO₃Nt
33 as covariables ($r = 0.74$ and RMSE = 1.18) outperformed ordinary kriging ($r = 0.18$ and
34 RMSE = 1.74), regression kriging with the sample position as a predictor ($r = 0.49$ and
35 RMSE = 1.55) and cokriging with SOct as a covariable ($r = 0.58$ and RMSE = 1.44). The
36 predictions of the three kriging interpolation methods for the total N₂O emissions of 4.0 ha
37 tea field ranged from 148.2 to 208.1 g N d⁻¹, based on the 30 min snapshots obtained during

38 the wet season. Our findings suggested that to accurately estimate the total N₂O emissions
39 over a region, the environmental variables (e.g., soil properties) and the current land use
40 pattern (e.g., tea row transects in the present study) must be included in spatial interpolation.
41 Additionally, compared with other kriging approaches, the cokriging prediction approach
42 showed great advantages in being easily deployed, and more importantly providing accurate
43 regional estimation of N₂O emissions from tea-planted soils.

44

45 **Introduction**

46 According to the latest data, which show rapid increases in their atmospheric concentrations
47 (IPCC, 2013), nitrous oxide (N₂O), carbon dioxide (CO₂) and methane (CH₄) are three major
48 greenhouse gases in the atmosphere that significantly contribute to global warming. Among
49 these major greenhouse gases, N₂O has a very high radiative forcing per unit mass (265-fold
50 stronger than CO₂ on a 100 year horizon) and plays an important role in ozone depletion in
51 the stratosphere (Ravishankara et al., 2009). The primary sources of N₂O are from agriculture
52 development and the subsequent increased use of chemical N fertilizers (Ambus and
53 Christensen, 1994; Mosier et al., 1996, 1998; Yanai et al., 2003; Tokuda and Hayatsu, 2004;
54 Akiyama et al., 2006; Ravishankara et al., 2009). Agricultural soils produce 2.8 (1.7–4.8) Tg
55 of N₂O-N yr⁻¹ (IPCC, 2013). The N₂O is emitted from soils via the microbial processes of
56 nitrification under aerobic conditions and denitrification under anaerobic conditions
57 (Firestone and Davidson, 1989; Wrage et al., 2004). The magnitude of soil N₂O emissions is
58 highly variable and strongly influenced by changes in environmental conditions.

59 Among the different agricultural soils, tea-planted soils are important sources of N₂O that
60 are rapidly attracting attention due to recent large increases in the number of tea plantations
61 and large N fertilizer inputs ([Akiyama et al., 2006](#); [Lin and Han, 2009](#); [Fu et al., 2010, 2012](#);
62 [Hirono and Nonaka, 2012](#); [Han et al., 2013](#); [Li et al., 2013](#)). In China, the total tea-planted
63 area was approximately 2.10 million ha (mostly distributed in Fujian, Anhui, Zhejiang and
64 Hunan) in 2013 ([NBSC, 2014](#)). Compared with other agricultural soils, tea-planted soils
65 provide optimal conditions (e.g., low soil pH, high temperature and ample moisture) for
66 microbes to emit significant amounts of N₂O ([Hayatsu, 1993](#); [Venterea and Rolston, 2000](#); [Li](#)
67 [et al., 2013](#)). However, because few measurements of N₂O emissions from tea-planted soils
68 have been reported in China ([Fu et al., 2012](#); [Li et al., 2013](#); [Han et al., 2013](#)), it is difficult to
69 conduct precise spatial and temporal evaluations of N₂O emissions from tea-planted soils. To
70 estimate the N₂O emissions from tea-planted soils accurately and to understand the roles that
71 tea plantations play in global warming, it is necessary to investigate the spatial and temporal
72 patterns and related mechanisms of N₂O emissions from tea fields. This information will lead
73 to the development of effective land management options for mitigating N₂O emissions from
74 a significant source, tea plantation.

75 The N₂O fluxes have large spatial variability in agricultural soils ([Konda et al., 2008](#),
76 [2010](#); [Meda et al., 2012](#); [Li et al., 2013](#)). Many previous studies in tea fields have found
77 pronounced seasonal fluctuations in N₂O fluxes, with higher N₂O emissions during the wet
78 season than during the dry season ([Fu et al., 2012](#); [Han et al., 2013](#)). The seasonal and spatial
79 variability of N₂O emissions significantly contributes to the uncertainty when estimating the

80 contributions of subtropical tea-planted ecosystems to N₂O flux. Moreover, most of our
81 knowledge regarding seasonal changes and the spatial variability of N₂O fluxes is based on a
82 small number of measurements taken from tea-planted soils. [Li et al. \(2013\)](#) investigated the
83 spatial structure of N₂O fluxes for tea-planted soils during the dry season in October 2010
84 and found that the spatial distribution of the N₂O fluxes was primarily associated with field
85 elevation ($r = -0.42$, $p < 0.001$). The other soil properties (e.g., soil organic carbon, soil water
86 and soil mineral nitrogen) were not significantly related to N₂O flux. To obtain a more
87 accurate evaluation of the interannual variability of N₂O emissions from tea-planted soils, a
88 study on the spatial structure and distribution of N₂O emissions during a wet season (in
89 contrast to the dry season) is necessary.

90 To understand the structure of the spatially distributed data and to predict the N₂O fluxes
91 at the unsampled locations, geostatistical analyses can be useful ([Goovaerts, 1997](#); [Webster
92 and Oliver, 2001](#)). Geostatistics provide statistical tools for describing the quantitative spatial
93 variability of field observations for the accurate mapping and planning of rational sampling
94 schemes that efficiently utilize the available labor ([Webster, 1985](#)). Several geostatistical
95 methods are used to examine the spatial variability of N₂O fluxes, including simple kriging
96 (SK), ordinary kriging (OK), regression kriging (RK) and cokriging (CK). The most
97 commonly used method is OK ([Clemens et al., 1999](#); [Röver et al., 1999](#); [Mathieu et al., 2006](#);
98 [Konda et al., 2008, 2010](#)), which uses the derived theoretical semivariogram models to
99 interpolate the spatial distribution of N₂O fluxes. However, research has demonstrated that
100 RK and CK approaches, which use related auxiliary variables, improve the prediction

101 accuracy (Goovaerts, 1997; Webster and Oliver, 2001; Hengl et al., 2004). The RK method
102 combines multiple regressions, including linear regressions, generalized linear models,
103 generalized added models and regression tree models, with the auxiliary variables used for
104 kriging (Odeh et al., 1994). In the RK method, linear regressions are commonly used. The
105 CK approach uses correlations that may exist between the predicted variables and other more
106 easily measured variables. These variables can be measured at the same points as the
107 predicted variable, at other points, or at both. Compared with the RK approach, the CK
108 approach is commonly applied when the measurement of a covariable is less expensive than
109 the cost of a predicted variable (Stein et al., 1988; Odeh et al., 1995). In addition to the
110 feature correlation as a criterion for selecting covariables, the CK approach also requires that
111 both of the predicted variable and covariables have similar spatial structures (Odeh et al.,
112 1994). In this study, we used three interpolation methods (OK, RK and CK) to estimate the
113 spatial distribution of N₂O fluxes in a tea field.

114 In contrast with the dry season, the spatial variability of the N₂O emissions was
115 investigated during the wet season in April 2012 from the same tea-planted catchment that
116 was studied by Li et al. (2013). The catchment consisted of a completely independent
117 hydrological system. Thus, the spatial distribution of the N₂O emissions within the catchment
118 was expected to have intrinsic characteristics. The objectives of this study were to (i) evaluate
119 the spatial variability of N₂O emissions from soils planted with tea in subtropical central
120 China during the wet season, (ii) determine the key environmental factors controlling N₂O
121 emissions, and (iii) assess the prediction efficiency of three kriging interpolation methods.

122

123 **2. Materials and Methods**

124 **2.1 Site description**

125 The field experiment was conducted in a small catchment (4.0 ha) in Jinjing, Changsha, in
126 Hunan province, China (28°32'50"N and 113°19'58" E and elevation 90 to 111 m) (Fig. 1).

127 The region has a subtropical monsoon climate with a mean annual air temperature of 17.5°C
128 and a mean annual precipitation of 1400 mm (average from 1979 to 2012). The site had four
129 distinct seasons: spring (February to April), summer (May to July), autumn (August to
130 November), and winter (December to January). On average, 70% of the annual precipitation
131 occurred in April, May and June. The daily air temperature and precipitation for 2012 were
132 recorded by an automatic weather station (Intelimet A, IMET-ADV2, Dynamax, USA)
133 located next to the studied catchment (Fig. 2). The soil of the catchment was a Haplic Alisol
134 (FAO/UNESCO soil taxonomy) that was derived from a granitic parental material. Tea
135 (*Camellia sinensis L., cv. Baihaozao*) was contour-planted 10 years ago using an inter-row
136 spacing of 0.5 m in the catchment.

137

138 *<Insert Fig. 1 & Fig. 2 near here>*

139

140 **2.2 Sampling positions**

141 In the 4.0 ha tea-planted catchment, 1964 evenly-distributed points with plane coordinates
142 and elevation values and 456 centerlines of tea tree row were recorded by locally calibrated
143 differential Geographic Positioning System (DGPS) receiver (Sanding Southern Survey Co.,

144 China), and then were used to develop the local DEM and land use data (at a spatial
145 resolution of 0.1 m, respectively, as shown in [Fig. 1c and d](#)). The land use data showed the
146 four positions where the chambers were placed, including the inter-row, fertilization point,
147 under tea tree and in tea tree row, as described in [Li. et al. \(2013\)](#). The spatial positions of the
148 gas sampling points in a 15 m × 15 m regular grid over the catchment were originally
149 determined using a DGPS receiver on 20 April 2012. Some of the chamber positions were
150 slightly adjusted (because of a lack of space in the tea tree rows or to avoid roads and
151 trenches). Thus, the chambers were placed in one of four locations mentioned above ([Fig. 1d](#)).
152 Overall, 147 sampling points were determined, and the Euclidean distances between each
153 point and its nearest neighbors ranged from 14.6 m to 16.7 m. The x-y coordinates, the gas
154 sampling position information (the inter-row, fertilization point, under tea tree and in tea tree
155 row along tea row transects), and the elevations at the sampling points were recorded.

156

157 **2.3 Gas and soil properties measurements**

158 Gas and soil samples were collected at each grid point on 22 April 2012 using a closed mini
159 chamber technique. A mini chamber set was composed of PVC and had two parts (base and
160 chamber). The base was 0.15 m in diameter and 0.05 m high. The chamber was 0.15 m in
161 diameter and 0.15 m high, and was equipped with rubber septa on the top for gas sampling. In
162 the field operation, the base was gently inserted vertically into the soil on 20 April 2012, and
163 the chamber was clipped on the base with the sponge seals in between to stop gas leaking
164 before gas sampling on 22 April 2012. Therefore, the effective static chambers volume was

165 equal to the chamber volume of 0.002651 m³. Gas samples were collected from the
166 headspace between 10 and 10.30 a.m. For simultaneous sampling, 25 skilled gas sampling
167 persons helped to accomplish the field sampling. Each person only took care of one column
168 containing 4 to 8 sampling positions (see Fig. 1), and started sampling at the same time of 10
169 a.m. At each point, three gas sample replicates were collected from the headspace into
170 pre-evacuated 12 mL vials (Exetainers, Labco, UK) at 0 and 30 min after the chamber body
171 was clipped. After collecting the gas samples, the air temperature in each chamber was
172 measured for subsequent correction of the flux calculation, and then three replicate soil cores,
173 0.05 m in diameter and 0.20 m in depth, were collected from the soils inside the mini
174 chambers. Soil samples were put straight into clean zip-lock bags for avoiding soil moisture
175 loss, and quickly transported back to the laboratory in thermal insulation boxes and stored in
176 a refrigeration room at 4 °C for preventing any microbial activity (such as mineralization,
177 nitrification and denitrification). The N₂O concentrations of the gas samples were analyzed
178 using a gas chromatograph (Agilent 7890A, Agilent, USA) that was fit with a ⁶³Ni-electron
179 capture detector and an automatic sample injector system. The N₂O fluxes (FLUX30, g N ha⁻¹
180 d⁻¹) were calculated as described by Li et al. (2013). The soil physical/chemical properties
181 determined by using fresh soil, e.g., the soil ammonium content (NH₄N), soil nitrate content
182 (NO₃N), soil dissolved organic carbon content (DOC), soil volumetric water content (SWC),
183 and soil bulk density (BD), were measured within three days after sampling, while those
184 using air-dried soil, e.g., total soil nitrogen content (TSN), soil organic carbon content (SOC)
185 and soil clay/silt/sand content (CLAY, SILT and SAND), were determined within two weeks

186 after the field work.

187

188 **2.4 Data analyses**

189 The descriptive statistical and geostatistical analyses were performed using R ([R](#)

190 [Development Core Team, 2014](#)) with the `gstat` package ([DGUU, 2010](#)).

191 Descriptive statistical analyses were used to determine the mean, median, minimum and
192 maximum values, SD, coefficient of variation (CV), and skewness of the original and
193 logit-transformed data. These analyses were based on the four chamber placement positions.
194 Because the FLUX30, NH4N, NO3N, SOC, TSN and SWC data were highly skewed, these
195 values were transformed by using a logit function ([Hengl et al., 2004](#)). The transformed
196 variables were named FLUX30t, NH4Nt, NO3Nt, SOct, TSNt and SWCt. Using a Pearson's
197 correlation, the relationships between FLUX30t, NH4Nt, NO3Nt, SOct, TSNt, SWCt, DOC,
198 BD, SAND, SILT, and CLAY were tested. The significance of the differences in the FLUX30t
199 and environmental factors (NH4Nt, NO3Nt, SOct, TSNt and DOC) between any two of the
200 different chamber positions along the entire tea-tree row transect were evaluated using the
201 Tukey's Honest Significant Difference method.

202 In the geostatistical analyses, an experimental semivariogram of FLUX30t was
203 calculated, and the theoretical semivariogram models were fit. The ratio of the partial sill to
204 the total sill was used as an index of spatial dependence. [Armstrong \(1998\)](#) stated that a
205 variable with a higher ratio of partial sill to sill and a longer semivariogram range were more
206 structured. The spatial distribution of FLUX30t across the catchment was predicted using

207 three kriging interpolation methods (OK, RK and CK). These data were transformed back to
208 the original scale of FLUX30 for mapping. The Leave-One-Out cross-validation method was
209 used to evaluate the accuracy of interpolating FLUX30t using the three different kriging
210 methods.

211

212 **3. Results**

213 **3.1 Exploratory data analyses**

214 In the 4.0 ha tea-planted catchment, the N₂O fluxes during the 30-min one-time
215 measurements performed on 22 April 2012 ranged from -1.73 to 1,659.11 g N ha⁻¹ d⁻¹, with a
216 median value of 27.56 g N ha⁻¹ d⁻¹ and a CV of 234.7 % (Table 1). The N₂O flux data were
217 positively skewed (Table 1 and Fig. 3a), and their logit-transformations were approximately
218 normally distributed (Table 1 and Fig. 3b). From Table 3, the logit-transformed N₂O fluxes
219 (FLUX30t) were the highest in the fertilization points, and the differences in the FLUX30t
220 values among the chamber placement positions were statistically significant ($p < 0.001$).

221

222 *<Insert Table 1 & Fig. 3 near here>*

223

224 The ELEVATION, BD, DOC, SWC, SAND, SILT, and CLAY were approximately
225 normally distributed, with skewness values of less than 1 (Table 1). Additionally, DOC
226 displayed a moderate CV of 34.6 %, and the other variables had lower CVs (4.1–23.8 %). The
227 NH₄N, NO₃N, SOC and TSN were positively skewed, and the logit-transformations (NH₄Nt,

228 NO₃Nt, SO_Ct and TSNt) had approximately normal distributions (Table 1). The NH₄N and
229 NO₃N had very high CVs (190.8 % and 141.6 %, respectively), and the SOC and TSN had
230 moderate CVs (50.1 % and 38.3 %, respectively).

231 The NH₄Nt, NO₃Nt, SO_Ct, TSNt and SWC were significantly correlated with the N₂O
232 fluxes (Fig. 5), and the NH₄Nt, NO₃Nt and TSNt had strong positive relationships with N₂O
233 ($r = 0.71, 0.70$ and 0.57 , respectively, $p < 0.001$). The N₂O emissions and some soil
234 properties (NH₄N, NO₃N, SOC, TSN and SWC) in the fertilization points were significantly
235 different ($p < 0.001$) from the other three chamber placement positions (Fig. 6). These
236 variables were used as auxiliary covariables for the CK approach.

237

238 *<Insert Fig. 4 & Fig. 5 near here>*

239

240 **3.2 Spatial variability of N₂O emissions and related environmental factors**

241 Because most of the soil properties were significantly correlated with the chamber placement
242 positions, two types of semivariogram models were calculated for the N₂O and soil
243 parameters (correlated with N₂O fluxes) in the wet season (Table 2). The FLUX30t exhibited
244 strong spatial autocorrelation and was characterized by an exponential semivariogram model,
245 a theoretical distance parameter of 8.40 m (equivalent to an effective range of 25.2 m) and a
246 zero nugget. The NH₄Nt, SWCt, SAND and SILT showed almost no spatial dependency,
247 while NO₃Nt and TSNt demonstrated weak spatial dependency with a range parameter of
248 91.9 and 58.0 m, respectively (equivalent to an effective range of 163.7 and 102.6 m,

249 respectively).The SOCt exhibited a moderate spatial dependency within 93.0 m. By
250 detrending the influence of the chamber placement position, large changes in the
251 semivariogram models occurred regarding the above variables. Although the semivariograms
252 of the regression residuals of FLUX30t, NH4Nt, NO3Nt and SOCt were best-fit with the
253 same semivariogram model (exponential) with a similar range of 17.4 m (equivalent to an
254 effective range of 52.1 m), the spatial dependencies of those variables were different (Table
255 2). Of the soil properties, only SOCt had a similar spatial structure to FLUX30t when the
256 influence of the chamber placement position was detrended (Table 2). Based on these
257 correlation analyses and spatial variability analyses, the covariables for the CK method were
258 determined.

259

260 *<Insert Table 2 near here>*

261

262 **3.3 Spatial interpolation of N₂O emissions by three methods**

263 Three spatial interpolation methods were used in this study to predict the spatial distribution
264 of N₂O emissions from tea soils in the catchment. In the first method, the derived theoretical
265 semivariogram model for FLUX30t that is presented in Table 2 was used for the OK
266 prediction. In the second method, RK was used and the chamber placement position was
267 identified as the auxiliary regression predictor. Thus, the semivariogram of the regression
268 residuals of FLUX30t were calculated and best-fit with the theoretical semivariogram model
269 shown in Fig. 6. In the third method, CK involved two groups of covariables. As described

270 previously, because SOct (detrending the influence of chamber placement position) showed a
271 similar spatial structure to FLUX30t (detrending the influence of chamber placing position), a
272 CK process was performed using SOct as the covariable. Firstly, the direct and
273 cross-semivariograms of FLUX30t and SOct (detrending the influence of the chamber
274 placement position) were calculated and best-fit with a linear model for co-regionalization
275 (LMC). Next, the fitted LMC was used to predict the spatial surface of N₂O emissions.
276 Because NH₄Nt and NO₃Nt were significantly correlated with FLUX30t (Fig. 5), a second
277 CK with NH₄Nt and NO₃Nt as the covariables was processed, similarly to that of the CK
278 with SOct. However, these covariables had different spatial structures (Table 2). As reflected
279 by the lower root mean squared error (RMSE) and higher *r* values (Table 4), the CK method
280 performed better than the other spatial interpolation methods. Furthermore, the CK with
281 NH₄Nt and NO₃Nt as two covariables outperformed the CK with SOct as the covariable.

282

283 *<Insert Figs.6-9 near here>*

284

285 As shown in Fig. 9, the surface map for the spatial distribution of N₂O emissions
286 interpolated by OK was rougher than the maps obtained from the other interpolation
287 approaches. The kriging standard deviation maps were showed in Fig. 10, and clearly
288 indicated that the RK and CK methods with lower kriging standard deviations outperformed
289 the OK method with higher kriging standard deviations. The four kriging interpolations of
290 OK, RK, CK with SOct as the covariable and CK with NH₄Nt and NO₃Nt as the covariables

291 were able to predict that the total amount of N₂O emissions in the tea fields during the wet
292 season were 208.1 g N d⁻¹, 148.2 g N d⁻¹, 149.7 g N d⁻¹ and 150.5 g N d⁻¹, respectively. From
293 the performance evaluations of the four spatial interpolations, the total N₂O emissions from
294 the tea field on 22 April 2012 during the wet season were approximately 150 g N d⁻¹.

295

296 *<Insert Fig. 10 near here>*

297

298 **Discussion**

299 **4.1 Seasonal differences of N₂O fluxes in the red soil planted with tea**

300 The N₂O emissions from soils have obvious seasonal fluctuations, with emissions that are
301 significantly higher during the wet season than during the dry season (Konda et al., 2010). To
302 understand the seasonal changes in the spatial structures of N₂O fluxes, we compared the
303 N₂O emissions between the wet (this study) and dry (Li et al., 2013) seasons. In general, the
304 mean, SD and CV (102.24, 239.96 g N ha⁻¹ d⁻¹ and 234.7 %, respectively) of the N₂O fluxes
305 in the wet season were all higher than those (2.88, 8.94 g N ha⁻¹ d⁻¹ and 152.0 %, respectively)
306 during the dry season (Table 3). Furthermore, in contrast with the dry season, the N₂O fluxes
307 during the wet season were significantly different among the four chamber placement
308 positions, with the highest fluxes occurring at the fertilization points and the inter-row
309 positions (Table 3). During the wet season, the high N₂O fluxes at the fertilization points and
310 the inter-row positions resulted from the high soil moisture, due to more rainfall, and from
311 the fertilization that occurred on 19 February 2012 (Fig. 2). The soil N and the soil organic C
312 availability are directly increased by the application of chemical and organic N fertilizers.

313 The additional in the available C and N supplied by fertilization resulted in increased soil
314 microbial activity, which stimulated the nitrification and denitrification processes that
315 contribute to soil N₂O emissions (Davidson et al., 1993; Kiese et al., 2003; Werner et al.,
316 2007).

317

318 *<Insert Table 3 near here>*

319

320 **4.2 Spatial structure of N₂O emissions from red soils planted with tea**

321 Soil type, topography and land management (fertilization, tillage and irrigation) are the
322 primary factors that affect the spatial structures of N₂O emissions (Folorunso and Rolston,
323 1984; Clemens et al., 1990; Velthof et al., 1996; Konda et al., 2008). During the wet season,
324 the N₂O fluxes showed a strong spatial dependence (with a range of approximately 25.3 m)
325 that was similar to the dry season range of approximately 28.0 m in the tea-planted fields (Li
326 et al., 2013). These results indicated that the spatial dependence of N₂O fluxes at the current
327 spatial sampling scale was comparable between seasons. Our findings for a fertilized tea field
328 were similar to those of Konda et al. (2010) for a tropical forest. However, these results
329 contrasted those of many previous investigations for agricultural fields, including winter
330 wheat (Ball et al., 1997; Clemens et al., 1999; Röver et al., 1999; Mathieu et al., 2006),
331 summer maize (Clements et al., 1999), onion (Yanai et al., 2003), and grassland (Ambus and
332 Christensen, 1994; Velthof et al., 1996; van den Pol-van Dasselaar et al., 1998; Turner et al.,
333 2008) fields, in which the N₂O flux presented no, weak or moderate spatial dependence. This

334 discrepancy primarily occurred because of the unique geographical characterization and land
335 management of the tea plantation. Compared with other agricultural fields in flat areas, tea
336 fields are always distributed in hills or mountains. Therefore, the contributions of the
337 topography to the spatial dependence of the N₂O flux were strong (Li et al., 2013).
338 Additionally, tea is a perennial plant. Thus, apart from fertilization and weeding, the soil
339 disturbance in tea fields is always very low.

340 During the dry season, the topography (elevation) had a significant effect on the spatial
341 pattern of N₂O fluxes in the tea-planted fields (Li et al., 2013). Similar spatial patterns of N₂O
342 fluxes with topography were also observed in forest soils (Van Kessel et al., 1993; Konda et
343 al., 2010). Theoretically, the SWC varies with the topography and affects the spatial pattern
344 of N₂O fluxes by controlling the conditions for soil nitrification and denitrification (Firestone
345 and Davidson, 1989; Wrage et al., 2004). Although the SWC had no relationships with N₂O
346 and elevation during the dry season (Li et al., 2013), a correlation existed in the present study
347 (Fig. 5). The microstructures of the tea tree-row transect and the land management practices
348 of tea production were the primary influences on the spatial pattern of soil water in the
349 tea-planted fields (Li et al., 2013). During the wet season, fertilization contributed to the
350 spatial pattern of N₂O fluxes in the tea-planted fields, with the highest averaged fluxes at the
351 fertilization sites (198.81 g N ha⁻¹ d⁻¹) (Table 3). Fertilization resulted in similar spatial
352 patterns of N₂O fluxes in other agricultural soils (Ball et al., 1997; Clements et al., 1999;
353 Röver et al., 1999; Mathieu et al., 2006; Yanai et al., 2003).

354 In view of the analysis of the primary factors that affected the spatial pattern of N₂O
355 fluxes, we detrended the influences of the environmental factors when the N₂O flux
356 semivariograms were calculated to more deeply explore the spatial structures of the N₂O
357 emissions in the tea-planted fields. For example, during the dry and wet seasons, the spatial
358 influences of elevation (Li et al., 2013) and chamber placement position, respectively, were
359 detrended when computing the N₂O flux semivariograms. Because the relationship between
360 chamber placement position and N₂O flux was more relevant than the relationship between
361 elevation and N₂O flux, the effect of detrending the influence of chamber placement position
362 during the wet season was more obvious than that of detrending the influence of elevation
363 during the dry season (Li et al., 2013). This effect was also reflected in the evaluation of the
364 performance of the RK method for the wet and dry seasons (Table 4).

365

366 **4.3 Spatial interpolations of N₂O emissions by three methods**

367 The three interpolation methods (OK, RK and CK) were used to predict the spatial
368 distributions of N₂O emissions from the red soils planted with tea during dry (Li et al., 2013)
369 and wet seasons (this study). However, these three methods resulted in significantly different
370 performances between the dry and wet seasons (Table 4). We conducted comparative
371 analyses for the performance of the three interpolation methods using two aspects: different
372 seasons and different methods. Firstly, the OK method performed better when predicting the
373 spatial distribution of N₂O fluxes for the dry season relative to the wet season. Because the
374 OK method directly used the fitted theoretical semivariogram model of the target variable to

375 predict the spatial distribution, its performance reflected the predictive ability of the original
376 data (Goovaerts, 1997). During the wet season, more factors (e.g., NH₄N, NO₃N, SOC, TSN
377 and SWC) influenced the spatial distributions of the N₂O fluxes than the dry season (Table 2
378 and Fig. 5). The values of the original data were concealed. Thus, other sophisticated kriging
379 methods, such as RK and CK, which reconcile the relationships between N₂O fluxes and
380 environmental factors, could be useful. The RK method performed better when elevation was
381 used as an auxiliary regression predictor during the dry season than when the chamber
382 placement position was used during the wet season (Table 4). This finding primarily occurred
383 because the chamber placement position was a categorical variable with a lower regression
384 fitting ability than elevation, which was a continuous variable (Goovaerts, 1997). The
385 performances of the CK with two groups of covariables during the wet season were better
386 than those of the CK with three groups of covariables during the dry season (Table 4).
387 Particularly, the CK with strongly correlated covariables of NO₃N and NH₄N ($r = 0.70$ – 0.71
388 and $p < 0.001$) (Fig. 5) performed the best ($r = 0.74$ and RMSE = 1.04) (Table 4).

389 Secondly, by comparing the performances of the three interpolation methods, the RK and
390 CK methods, which are more sophisticated kriging technologies, performed better than the
391 OK method for the dry and wet seasons. Similar results were obtained by previous
392 researchers (Stein et al., 1988; Odeh et al., 1995; Goovaerts, 1997; Hengl et al., 2004). When
393 comparing the performances of RK and CK, no differences were observed for the dry season.
394 However, during the wet season, the CK significantly outperformed the RK (Table 4). Overall,
395 few attempts have been made to provide a good method for selecting interpolation methods

396 between RK and CK (Kontters et al., 1995; Odeh et al. 1995). Li et al. (2013) suggested that
397 RK was a good choice because of the performance of the two interpolation methods and the
398 difficulties encountered when applying CK. However, in this study, the CK method was
399 better than the RK method because of its high predictive performance (Table 4), its readily
400 available required covariables (e.g., NH4N, NO3N and SOC) at co-locations, and because
401 expensive surface data were not needed (e.g., DEM and land use data, which are required by
402 RK) (Goovaerts, 1997; Webster and Oliver, 2001). Our conclusions were similar to those of
403 many previous studies that found that CK was the most versatile and rigorous statistical
404 technique for estimating spatial points (Stein et al., 1988; Odeh et al., 1995; Webster and
405 Oliver, 2001). For the application of CK, the covariables must show a correlation with the
406 target variable and present a similar spatial structure as the target variable (Odeh et al., 1995;
407 Goovaerts, 1997; Webster and Oliver, 2001). Therefore, we further compared the effects of
408 the two groups of covariables for CK in this study. We found that CK method with NH4Nt
409 and NO3Nt (showed significant correlations with FLUX30t) as covariables outperformed the
410 CK method with SOct (presented a similar spatial structure to FLUX30t) as a covariable,
411 indicating that the feature correlation was more important than the similarity of the spatial
412 structure when selecting CK covariables. This finding can be regarded as a prerequisite for
413 selecting covariables for CK application.

414

415 *<Insert Table 4 near here>*

416

417 The three spatial interpolation methods predicted similar total N₂O emissions from the
418 tea-planted red soils in the 4.0 ha catchment on 30 October 2010 (in the dry season) and on
419 22 April 2012 (in the wet season), ranging from 21.2 to 22.1 g N d⁻¹ and from 148.2 to 208.1
420 g N d⁻¹ (Table 4), respectively. The predicted errors during the wet season were higher than
421 those of the dry season (Table 4). This result mainly occurred because fertilization was a
422 major factor that affected the N₂O emissions from the tea fields during the wet season.
423 Following fertilization, the horizontal and vertical movement of NH₄N and NO₃N in the
424 topsoil of the tea fields potentially produced the strong spatial heterogeneity of N₂O
425 emissions. In addition, it is possible that the variations in the availability of oxygen in the
426 soils was regulated by soil moisture, which determined the spatio-temporal heterogeneity of
427 N₂O emissions by inducing different degrees of soil nitrification and denitrification
428 (Davidson et al., 2000; Konda et al., 2010). Thus, spatial interpolation methods must be
429 chosen carefully to accurately estimate the spatial distribution of N₂O emissions when the
430 emissions are high and have strong spatial variability in the fields.

431

432 **5 Conclusions**

433 During the wet season of 2012, a 30-min one-time measurement of N₂O emissions from a 4.0
434 ha red-soil tea field in the subtropical region of central China were determined at 147 points.
435 The N₂O fluxes significantly varied with space. In addition, the N₂O fluxes were significantly
436 correlated with the NH₄N, NO₃N, SOC and TSN contents ($r > 0.27$ and $p < 0.001$). The
437 logit-transformed N₂O fluxes demonstrated a strong spatial dependency and were

438 characterized by an exponential semivariogram model with an effective range of 25.2 m.
439 Three spatial interpolation methods (OK, RK and CK) were used to predict the spatial
440 distribution of N₂O emissions. The RK and CK methods were relatively accurate for
441 predicting results. Although the N₂O emissions were much higher during the wet season than
442 in the dry season, the N₂O emissions exhibited similar spatial structure during both seasons.
443 Such a phenomenon was mainly attributed to the low soil disturbance (e.g., only fertilizing in
444 a very small proportion of area and weeding) in the tea field.

445 To effectively mitigate high N₂O emissions from the tea field soils, the biological and
446 chemical mechanisms of N₂O emissions must be deeply explored. In addition, the responsive
447 land management practices, such as biochar application, deep fertilization (under 20 cm), the
448 use of controlled-release fertilizers and ecological engineering, must be recommended and
449 deployed, especially during the wet season.

450

451 **Acknowledgements**

452 The National Basic Research Program of China (2012CB417105) and the National Natural
453 Science Foundation of China (41171200) financially supported this research.

454 **References**

- 455 Akiyama, H., Yan, X. Y., and Yagi, K.: Estimations of emission factors for fertilizer-induced
456 direct N₂O emissions from agricultural soils in Japan: Summary of available data, *Soil Sci.*
457 *Plant Nutr.*, 52, 774-787, 2006.
- 458 Ambus, P., and Christensen, S.: Measurement of N₂O emission from a fertilized grassland: an
459 analysis of spatial variability, *J. Geophys. Res.*, 99, 16557-16567, 1994.
- 460 Armstrong, M.: *Basic linear Geostatistics*, Springer Verlag, Berlin, 153 pp., 1998.
- 461 Ball, B. C., Horgan, G. W., Clayton, H., and Parker, J. P.: Spatial variability of nitrous oxide
462 fluxes and controlling soil and topographic properties, *J. Environ. Qual.*, 26, 1399-1409,
463 1997.
- 464 Clemens, J. Schillinger, M. P., Goldbach, H., and Huwe, B.: Spatial variability of N₂O
465 emissions and soil parameters of an arable silt loam - a field study, *Bio. Fert. Soils*, 28,
466 403-406, 1999.
- 467 Davidson, E. A., Matson, P. A., Vitousek, P. M., Riley, R., Dunkin, K., García-Méndez, G.,
468 and Maass, J. M.: Processes regulating soil emissions of NO and N₂O in a seasonally dry
469 tropical forest, *Ecology*, 74, 130-139, 1993.
- 470 Davidson, E. A., Keller, M., Erickson, H. E., Verchot, L. V., and Veldkamp, E.: Testing a
471 conceptual model of soil emissions of nitrous and nitric oxides, *Bioscience*, 50, 667-680,
472 2000.
- 473 DGUU (Department of Geography, Utrecht University): Introduction for Gstat, available at:
474 <http://www.gstat.org/index.html> (last access: 15 December 2010), 2010.

475 Firestone, M., and Davidson, E.: Microbial basis of NO and N₂O production and
476 consumption, in: Exchange of Trace Gases Between Ecosystems and the Atmosphere,
477 edited by: Andreae, M.O. and Schimel, D.S., John Wiley, Chichester, 7-21, 1989.

478 Folorunso, O. A., and Rolston, D. E.: Spatial variability of field measured denitrification gas
479 fluxes, *Soil Sci. Soc. Am. J.*, 48, 1214-1219, 1984.

480 Fu, X., Li, Y., Xiao, R., Tong, C., and Wu, J.: N₂O emissions from a tea field in subtropical
481 China. In: Proceedings of the 19th World Congress of Soil Science, Soil Solutions for a
482 Changing World, 1–6 August 2010, Brisbane (published on CDROM), 161-163, 2010.

483 Fu, X., Li, Y., Su, W., Shen, J., Xiao, R., Tong, C., and Wu, J.: Annual dynamics of N₂O
484 emissions from a tea field in southern subtropical China, *Plant Soil Environ.*, 58,
485 373-378, 2012.

486 Goovaerts, P.: *Geostatistics for Natural Resources Evaluation*, Oxford University Press, New
487 York, 483 pp., 1997.

488 Gorres, J. H., Dichiario, M. J., and Lyons, J. A.: Spatial and temporal patterns of soil
489 biological activity in a forest and an old field, *Soil Biol. Biochem.*, 30, 219-230, 1998.

490 Han, W., Xu, J., Wei, K., Shi, W., and Ma, L.: Estimation of N₂O emission from tea garden
491 soils, their adjacent vegetable garden and forest soils in eastern China, *Environ. Earth Sci.*,
492 70, 2495-2500, 2013.

493 Hayatsu, M.: The lowest limit of pH for nitrification in tea soil and isolation of an acidophilic
494 ammonia oxidizing bacterium, *Soil. Sci. Plant Nutr.*, 39, 219-226, 1993.

495 Hengl, T., Heuvelink, G. B. M., and Stein, A.: A generic framework for spatial prediction of
496 soil variables based on regression-kriging, *Geoderma*, 120, 75-93, 2004.

497 Hirono, Y., and Nonaka, K.: Nitrous oxide emissions from green tea fields in Japan:
498 contribution of emissions from soil between rows and soil under the canopy of tea plants,
499 *Soil. Sci. Plant Nutr.*, 58, 384-392, 2012.

500 IPCC: Climate change 2013: the physical science basis. Contribution of working group I, in:
501 Fourth assessment report of the intergovernmental panel on climate change, edited by:
502 Solomon S., Qin D., Manning, M., Chen Z., Marquis, M., Averyt, K.B., Tignor, M.,
503 Miller, H.L., Cambridge University Press, Cambridge, 996 pp., 2013.

504 ISM (Institute for Statistics and Mathematics): The R Project for Statistical Computing,
505 available at: <http://www.r-project.org/> (last access: 15 December 2010), 2010.

506 Kiese, R., Hewett, B., Graham, A., and Butterbach-Bahl, K.: Seasonal variability of N₂O
507 emissions and CH₄ uptake by tropical rainforest soils of Queensland, Australia. *Global*
508 *Biogeochem. Cy.*, 17, 1043, doi:10. 1029/2002GB002014, 2003.

509 Konda, R., Ohta, S., Ishizuka, S., Arai, S., Ansori, S., Tanaka, N., and Hardjono, A.: Spatial
510 structures of N₂O, CO₂, and CH₄ fluxes from *Acacia mangium* plantation soils during a
511 relatively dry season in Indonesia, *Soil Biol. Biochem.*, 40, 3021-3030, 2008.

512 Konda, R., Ohta, S., Ishizuka, S., Heriyanto, J., and Wicaksono, A.: Seasonal changes in the
513 spatial structures of N₂O, CO₂ and CH₄ fluxes from *Acacia mangium* plantation soils in
514 Indonesia, *Soil Biol. Biochem.*, 42, 1512-1522, 2010.

515 Li, Y., Fu, X., Liu, X., Shen, J., Luo, Q., Xiao, R., Li, Y., Tong, C., and Wu, J.: Spatial
516 variability and distribution of N₂O emissions from a tea field during the dry season in
517 subtropical central China, *Geoderma*, 193, 1-12, 2013.

518 Lin, Y., and Han, W.: N₂O emissions from different soils, *Chinese Journal of Tea Science*, 29,
519 456-464, 2009.

520 Mathieu, O., Lévêque, J., Hénault, C., Milloux, M. J., Bizouard, F., and Andreux, F.:
521 Emissions and spatial variability of N₂O, N₂ and nitrous oxide mole fraction at the field
522 scale, revealed with ¹⁵N isotopic techniques, *Soil Biol. Biochem.*, 38, 941-951, 2006.

523 Meda, B., Flechard, C. R., Germain, K., Robin, P., Walter, C., and Hassouna, M.:
524 Greenhouse gas emissions from the grassy outdoor run of organic broilers,
525 *Biogeosciences*, 9, 1493-1508, doi:10.5194/bg-9-1493-2012, 2012.

526 Mosier, A. R., Duxbury, J. M., Freney, J. R., Heinemeyer, O., and Minami, K.: Nitrous oxide
527 emissions from agricultural fields: assessment, measurement and mitigation. *Plant Soil*,
528 181, 95-108, 1996.

529 Mosier, A. R., Kroeze, C., Nevison, C., Oenema, O., Seitzinger, S., and van Cleemput, O.:
530 Closing the global N₂O budget: nitrous oxide emissions through the agricultural nitrogen
531 cycle, *Nutr. Cycl. Agroecosys.*, 52, 225-248, 1998.

532 NBSC (a): China Statistical Yearbook, annual publication, National Bureau of Statistics of
533 China, Beijing, 2014.

534 Odeh, I. O. A., McBratney, A. B., and Chittleborough, D. J.: Spatial prediction of soil
535 properties from landform attributes derived from a digital elevation model, *Geoderma*, 63,
536 197-214, 1994.

537 Odeh, I. O. A., McBratney, A. B., and Chittleborough, D. J.: Further results on prediction of
538 soil properties from terrain attributes: heterotopic cokriging and regression kriging,
539 *Geoderma*, 67, 215-226, 1995.

540 R Development Core Team: R: a language and environment for statistical computing. R
541 Foundation for Statistical Computing, 2014.

542 Ravishankara, A. R., Daniel, J. S., and Portmann, R. W.: Nitrous oxide (N₂O): the dominant
543 ozone-depleting substance emitted in the 21st century, *Science*, 326, 123-125, 2009.

544 Röver, M., Heinemeyer, O., Munch, J. C., and Kaiser, E. A.: Spatial heterogeneity within the
545 plough layer: high variability of N₂O emission rates, *Soil Biol. Biochem.*, 31, 167-173,
546 1999.

547 Stein, A., van Dooremolen, W., Bouma, J., and Bregt, A. K.: Cokriging point data on
548 moisture deficit. *Soil Sci. Soc. Am. J.*, 52, 1418-1423, 1988.

549 Tokuda, S. I., and Hayatsu, M.: Nitrous oxide flux from a large amount of nitrogen fertilizer
550 and soil environmental factors controlling the flux, *Soil. Sci. Plant Nutr.*, 50, 365-374,
551 2004.

552 Turner, D. A., Chen, D., Gellbally, I. E., Li, Y., Edis, R. B., Leuning, R., Kelly, K., and
553 Phillips, F.: Spatial variability of nitrous oxide emissions from an Australian irrigated
554 dairy pasture, *Plant soil*, 309, 77-88, 2008.

555 Van den Pol-van Dasselaar, A., Corré, W. J., Klemedtsson, A., Weslien, P., Stein, A.,
556 Klemedtsson, L., and Oenema, O.: Spatial variability of methane, nitrous oxide, and
557 carbon dioxide emissions from drained grasslands, *Soil Sci. Soc. Am. J.*, 62, 810-817,
558 1998.

559 Van Kessel, C., Pennock, D.J., and Farrell, R.E.: Seasonal-variations in denitrification and
560 nitrous oxide evolution at the landscape scale, *Soil Sci. Soc. Am. J.*, 57, 988-995, 1993.

561 Velthof, G. L., Jarvis, S. C., Stein, A., Allen, A. G., and Oenema, O.: Spatial variability of
562 nitrous oxide fluxes in mown and grazed grasslands on a poorly drained clay soil, *Soil*
563 *Biol. Biochem.*, 28, 1215-1225, 1996.

564 Venterea, R. T., and Rolston, D. E.: Mechanisms and kinetics of nitric and nitrous oxide
565 production during nitrification in agricultural soil, *Glob. Change Biol.*, 6, 303-316, 2000.

566 Webster, R.: Quantitative spatial analysis of soil in the field, in: *Advances in Soil Science*,
567 edited by: Stewart, B.A., Springer, New York, 1-70, 1985.

568 Webster, R., and Oliver, M. A.: *Geostatistics for Environmental Scientists*, John Wiley &
569 Sons, Chichester, 2001.

570 Werner, C., Kiese, R., and Butterbach-Bahl, K.: Soil-atmosphere exchange of N₂O, CH₄, and
571 CO₂ and controlling environmental factors for tropical rain forest sites in western Kenya,
572 *J. Geophys Res.*, 112, D03308, doi:10.1029/2006JD007388, 2007.

573 Wrage, N., Velthof, G. L., Laanbroek, H. J., and Oenema, O.: Nitrous oxide production in
574 grassland soils: assessing the contribution of nitrifier denitrification, *Soil Biol. Biochem.*,
575 36, 229-236, 2004.

576 Yanai, J., Lee, C. K., Umeda, M., and Kosaki, T.: Spatial variability of soil chemical
577 properties in a paddy field. *Soil Sci. Plant Nutr.*, 46, 473-482, 2000.

578 Yanai, J., Sawamoto, T., Oe, T., Kusa, K., Yamakawa, K., Sakamoto, K., Naganawa, T.,
579 Inubushi, K., Hatano, R., and Kosaki, T.: Atmospheric pollutants and trace gases: spatial
580 variability of nitrous oxide emissions and their soil-related determining factors in an
581 agricultural field, *J. Environ. Qual.*, 32, 1965-1977, 2003.

582

583 Table 1 Descriptive statistics of the N₂O fluxes and environmental factors.

Variable ^a	Mean	Minimum	Maximum	CV (%)	Skewness of the original data	Skewness of the logit-transformed data
FLUX30	102.24 ^b	-1.73	1,659.11	234.7	4.37	0.6
ELEVATION	80.64	74.25	87.96	4.1	0.04	-
BD	1.26	0.90	1.56	10.1	-0.28	-
DOC	185.56	43.70	424.14	34.6	0.75	-
NH4N	62.33	1.89	842.55	190.8	3.28	0.17
NO3N	21.54	0.48	135.29	141.6	1.85	0.28
SOC	13.33	5.11	52.52	50.1	2.27	-0.44
TSN	1.52	0.81	4.12	38.3	1.73	-0.01
SWC	0.33	0.19	0.47	16.6	0.07	-
SAND	39.73	16.98	63.79	23.8	0.02	-
SILT	47.15	26.78	64.17	16.1	-0.29	-
CLAY	13.12	8.68	21.68	21.5	1.00	-

584 ^aFLUX30 is the N₂O flux (g N ha⁻¹ d⁻¹); ELEVATION is the elevation (m); and BD, DOC,
585 NH4N, NO3N, SOC, TSN, SWC, SAND, SILT and CLAY are the soil bulk density (Mg m⁻³),
586 soil dissolved organic carbon (mg C kg⁻¹ soil), soil ammonium (mg N kg⁻¹ soil), soil nitrate
587 (mg N kg⁻¹ soil), soil organic carbon (g C kg⁻¹ soil), soil total nitrogen (g N kg⁻¹ soil),

588 gravimetric soil water ($\text{g H}_2\text{O g}^{-1}$ soil), soil sand particle (%), soil silt particle (%) and soil
589 clay particle (%) content, respectively, of the 0-20 cm of topsoil.

590 ^bThe median and standard deviation of the FLUX30 were 27.56 and $239.96 \text{ g N ha}^{-1} \text{ d}^{-1}$,
591 respectively.

592 Table 2 Semivariogram models for N₂O fluxes and the environmental factors.

Variable	Model	Nugget	Partial sill	Sill(nugget+ partial sill)	Distance Parameter (m)	Effective range (m)	Partial sill/sill
FLUX30t ^a	Exp	0	3.7186	3.7186	8.40	25.2	1.00
NH4Nt ^a	ND ^c	ND ^c	ND ^c	ND ^c	ND ^c	ND ^c	ND ^c
NO3Nt ^a	Ste	4.0794	0.6113	4.6907	91.92	163.7	0.13
SOct ^a	Sph	1.1198	0.7744	1.8942	92.96	93.0	0.41
TSNt ^a	Ste	1.0422	0.2816	1.3238	57.97	102.6	0.21
SWCt ^a	ND ^c	ND ^c	ND ^c	ND ^c	ND ^c	ND ^c	ND ^c
SAND ^a	ND ^c	ND ^c	ND ^c	ND ^c	ND ^c	ND ^c	ND ^c
SILT ^a	ND ^c	ND ^c	ND ^c	ND ^c	ND ^c	ND ^c	ND ^c
FLUX30t ^b	Exp	1.1911	2.0560	3.2471	17.36	52.1	0.63
NH4Nt ^b	Exp	2.0473	0.7185	2.7658	17.36	52.1	0.26
NO3Nt ^b	Exp	1.6241	1.1188	2.7429	17.36	52.1	0.41
SOct ^b	Exp	0.6043	1.0777	1.6820	17.36	52.1	0.64
TSNt ^b	Ste	0.9347	0.3114	1.2461	59.53	105.4	0.25
SWCt ^b	ND ^c	ND ^c	ND ^c	ND ^c	ND ^c	ND ^c	ND ^c
SAND ^b	ND	ND	ND	ND	ND	ND	ND
SILT ^b	ND	ND	ND	ND	ND	ND	ND

593 ND, not determined.

594 ^aSemivariogram models for the OK method.

595 ^bSemivariogram models for the RK method using the chamber placement position as the
596 auxiliary regression predictor.

597 ^cSpatial structures were not apparent.

598

599 Table 3 Statistics for N₂O fluxes during the dry and wet seasons.

Sample position	Mean	SD	Median	Max.	Min.	CV (%)
Dry season						
Inter-row (58)	5.15	4.95	4.09	22.43	-2.83	96.1
Fertilization point (50)	7.19	12.04	4.34	79.56	-6.42	167.4
Under tree (28)	3.58	2.91	2.36	10.28	0.68	81.3
In tree row (11)	5.95	10.38	3.98	52.17	-5.69	174.5
Wet season						
Inter-row (45)	101.69	287.23	27.56	1,659.11	-0.81	282.5
Fertilization point (45)	198.81	295.70	73.42	1,404.32	0.85	148.7
Under tree (22)	16.74	17.00	10.64	61.24	-1.73	101.6
In tree row (33)	28.30	38.34	14.72	177.08	0.19	135.5

600 The numbers in the parentheses represent the sample numbers for each chamber placement
 601 position.

602

603 Table 4 Cross-validations of the three different kriging interpolations for N₂O fluxes during
 604 the dry and wet seasons.

Method of spatial interpolation	Auxiliary variable	ME (no dimension)	RMSE (no dimension)	<i>r</i>	Predicted total N ₂ O emissions (g N d ⁻¹)
Dry season					
OK	-	0.0002	0.102	0.52	22.1 ^a
RK	ELEVATION	0.0008	0.098	0.57	21.1 ^a
CK	SOct	0.0006	0.103	0.51	22.0 ^a
CK	ELEV	0.0008	0.099	0.57	21.5 ^a
CK	SOct and ELEV	0.0009	0.098	0.57	21.2 ^a
Wet season					
OK	-	-0.0005	1.739	0.18	208.1
RK	POSITION	-0.0006	1.549	0.49	148.2
CK	SOct (POSITION)	0.0020	1.439	0.58	149.5
CK	NH4Nt (POSITION) and NO3Nt (POSITION)	0.0001	1.185	0.74	150.5

605 OK, RK and CK correspond to ordinary kriging, regression kriging and cokriging,
606 respectively; For the dry season campaign, ELEVATION, SOct and ELEV are the normalized
607 elevation, the normalized soil organic carbon content and the inverse of the normalized
608 elevation, respectively. For the wet season campaign, SOct, NH4Nt and NO3Nt are the
609 logit-transformations of soil organic carbon, soil ammonium and soil nitrate concentrations,
610 respectively. "POSITION" (in the parentheses) indicates the process of detrending the
611 influence of chamber placement position. The ME, RMSE, and r are the mean prediction
612 error, the root mean squared error (the mean squared deviation ratio of the prediction
613 residuals to the kriging standard errors), and the Pearson's correlation coefficient between the
614 observations and the predictions, respectively.

615 ^aThe predicted total N₂O emissions during the dry season were recalculated because the study
616 area changed from 4.8 ha to 4.0 ha for the wet season.

617

618 **Figure captions**

619

620 Figure 1. **(a, b)** Location and **(c, d)** digital elevation model and land use map of the tea
621 planted catchment. The red circles in **(c, d)** represent the sample points. The catchment is
622 located in Jinjing town, which is 70 km northeast of Changsha, the capital city of Hunan
623 Province, China.

624

625 Figure 2. Daily **(a)** air temperatures and **(b)** precipitation during 2012.

626

627 Figure 3. Histograms of **(a)** the original N₂O fluxes (FLUX30) and **(b)** the logit-transformed
628 N₂O fluxes (FLUX30t).

629

630 Figure 4. The Tukey's Honest Significant Difference analysis for FLUX30t, NH₄Nt, NO₃Nt,
631 SO₄t, TSNt and SWCt based on the four-chamber placement positions (R, inter-row; F,
632 fertilization point; U, under tea tree; and I, in the tea tree row).

633

634 Figure 5. Correlation matrix with the Pearson's correlation coefficients (*r*) of the N₂O fluxes
635 and the environmental factors. All of the variables in the correlation matrix are normally
636 distributed. FLUX30 represents the N₂O flux (g N ha⁻¹ d⁻¹); ELEVATION is the elevation (m);
637 and BD, DOC, NH₄N, NO₃N, SOC, TSN, SWC, SAND, SILT and CLAY are the soil bulk
638 density (Mg m⁻³), soil dissolved organic carbon (mg C kg⁻¹ soil), soil ammonium (mg N kg⁻¹

639 soil), soil nitrate (mg N kg^{-1} soil), soil organic carbon (g C kg^{-1} soil), total soil nitrogen (g N
640 kg^{-1} soil), gravimetric soil water ($\text{g H}_2\text{O g}^{-1}$ soil), soil sand particle (%), soil silt particle (%)
641 and soil clay particle (%) contents of the top 0-20 cm of the soil, respectively. Furthermore, *,
642 ** and *** represent the statistical significance at probability levels of 0.05, 0.01 and 0.001,
643 respectively. The lowercase letter t represents the logit transformation.

644

645 Figure 6. Semivariograms (open circles) and best-fitted models (solid lines) of the normal
646 logit-transformed N_2O fluxes (FLUX30t) (no dimension) for ordinary kriging (**a**) and the
647 regression residuals of FLUX30t (no dimension) with chamber placement position as the
648 predictor for regression kriging (**b**).

649

650 Figure 7. Direct and cross-semivariograms (open circles, detrending the influence of chamber
651 placement position for cokriging) and the best-fitted linear model of the co-regionalization
652 (solid lines) of the normal logit-transformed N_2O fluxes (FLUX30t) (no dimension) and the
653 normal SOC (SOCt, no dimension). The linear model of co-regionalization was characterized
654 by using the same range and different sills for its component models.

655

656 Figure 8. Direct and cross-semivariograms (open circles, detrending the influence of chamber
657 placement position for cokriging) and the best-fit linear model of co-regionalization (solid
658 lines) for the normal logit-transformed N_2O fluxes (FLUX30t) (no dimension), NH_4N
659 (NH_4Nt , no dimension) and NO_3N (NO_3Nt , no dimension). The linear model of

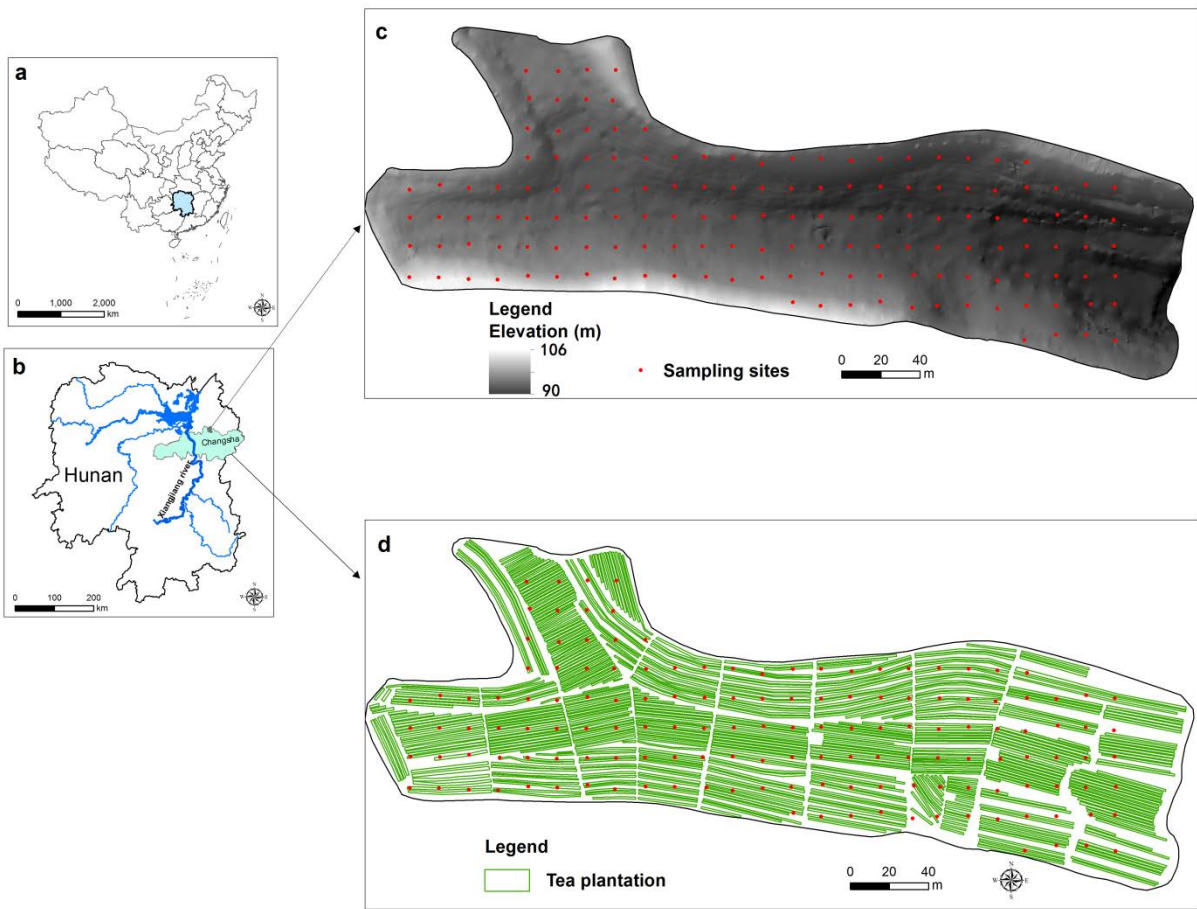
660 co-regionalization was characterized by the same range and different sills for its component
661 models.

662

663 Figure 9. Spatial distributions of the N₂O fluxes as predicted by **(a)** OK, **(b)** RK with
664 chamber placement position as the regression predictor, **(c)** CK with SOCt (with the influence
665 of chamber placement position detrended) as the covariable, and **(d)** CK with NH₄Nt (with
666 the influence of chamber placement position detrended) and NO₃Nt (with the influence of
667 chamber placement position detrended) as two covariables. Here, SOCt, NH₄Nt and NO₃Nt
668 represent the logit-transformed soil organic carbon, soil ammonium and soil nitrate content,
669 respectively.

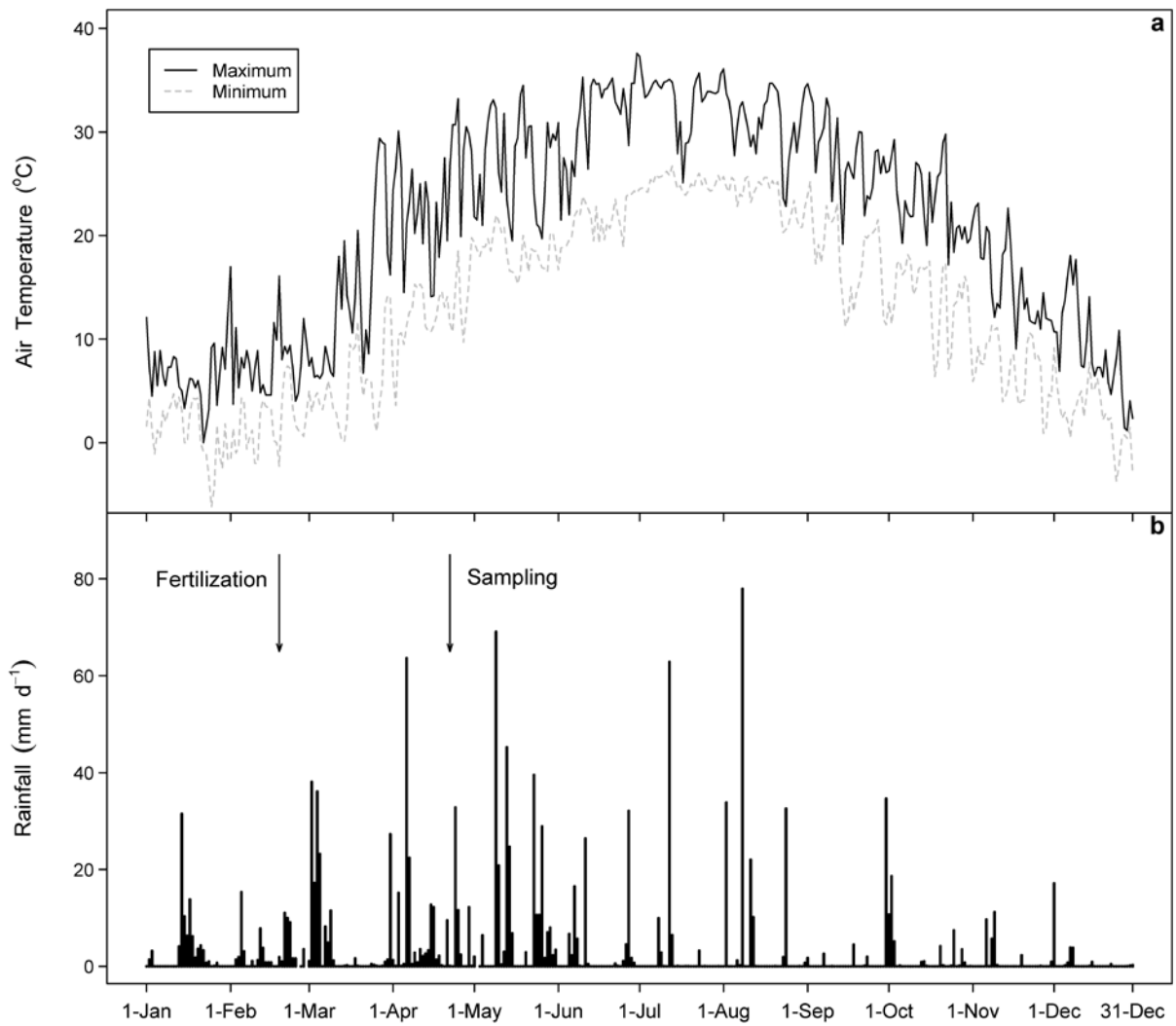
670

671 Figure 10. Spatial distributions of kriging standard deviations of the predicted N₂O fluxes by
672 **(a)** OK, **(b)** RK, **(c)** CK with SOCt as the covariable, and **(d)** CK with NH₄Nt and NO₃Nt as
673 two covariables.



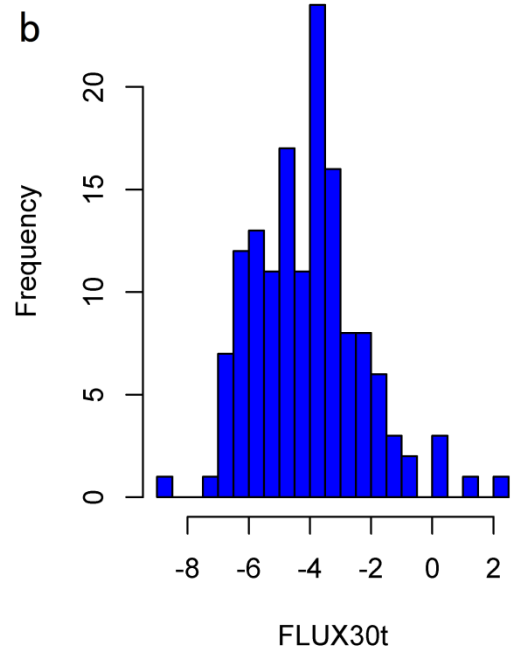
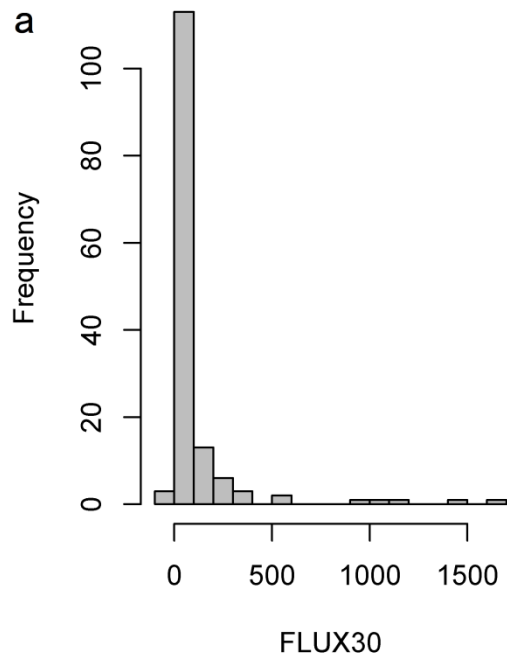
674

675 Figure 1



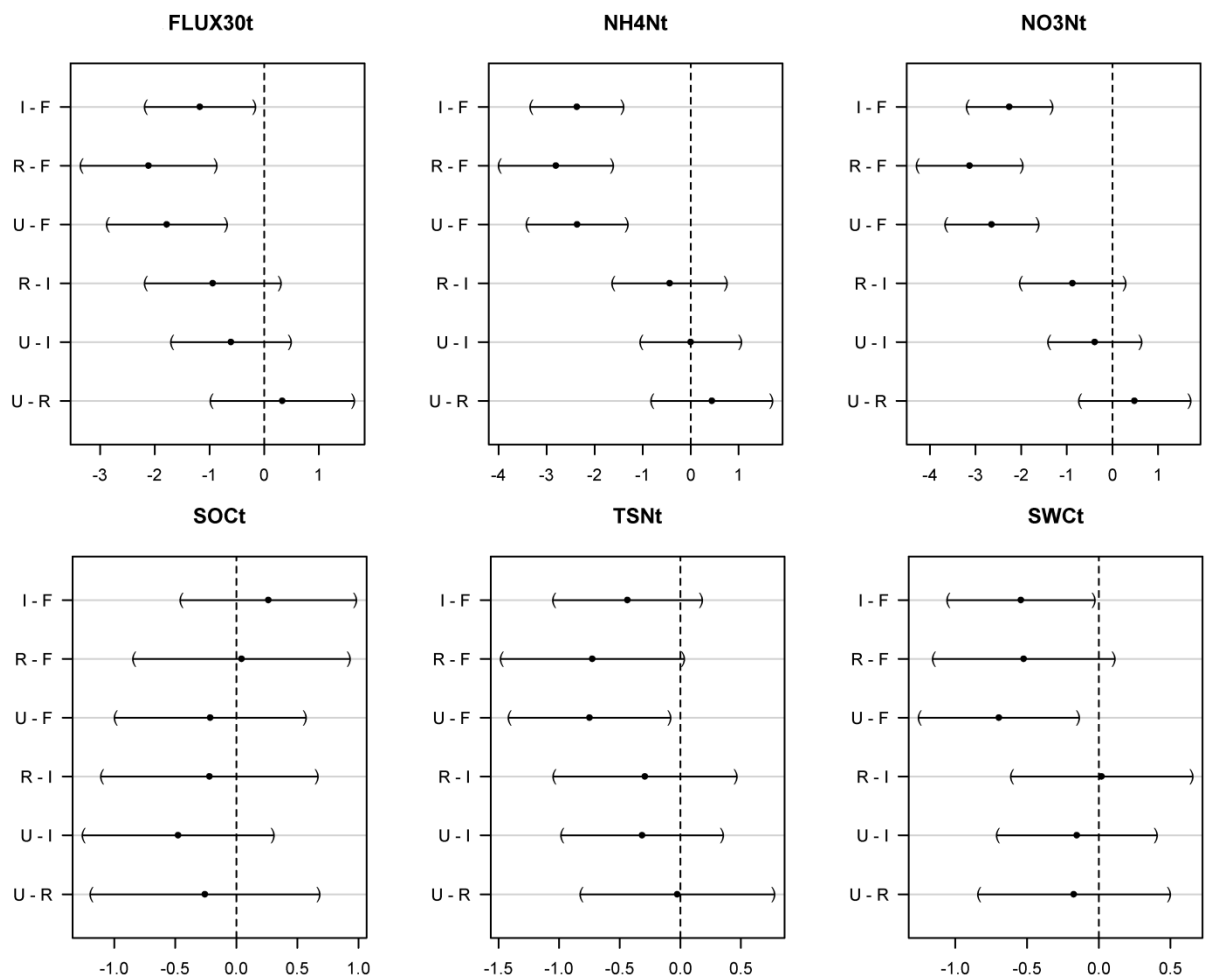
676

677 Figure 2



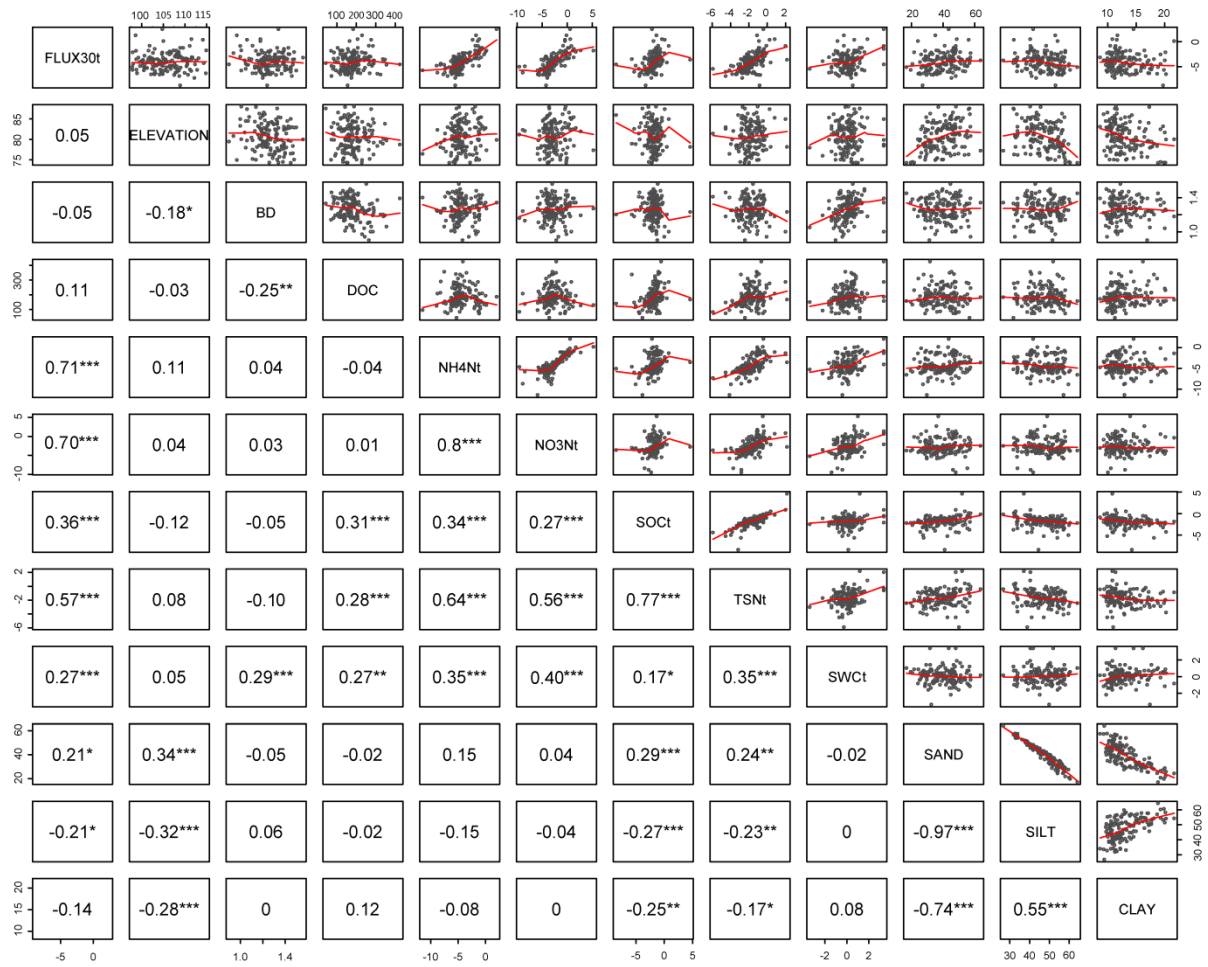
678

679 Figure 3



680

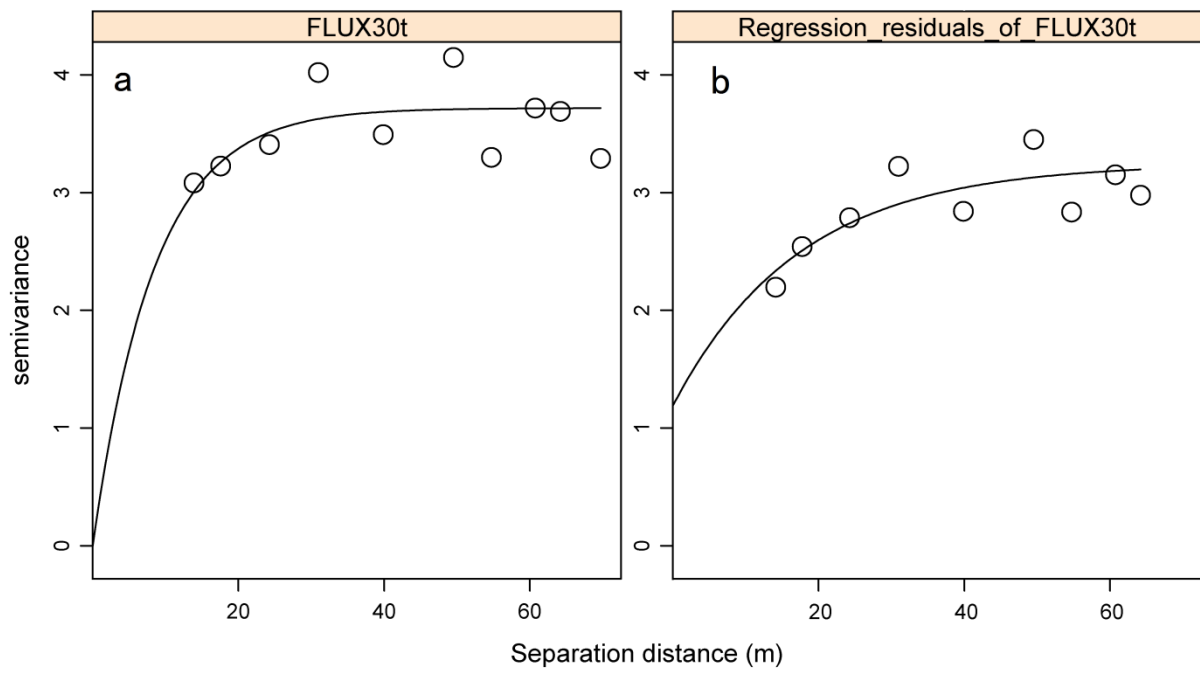
681 Figure 4



682

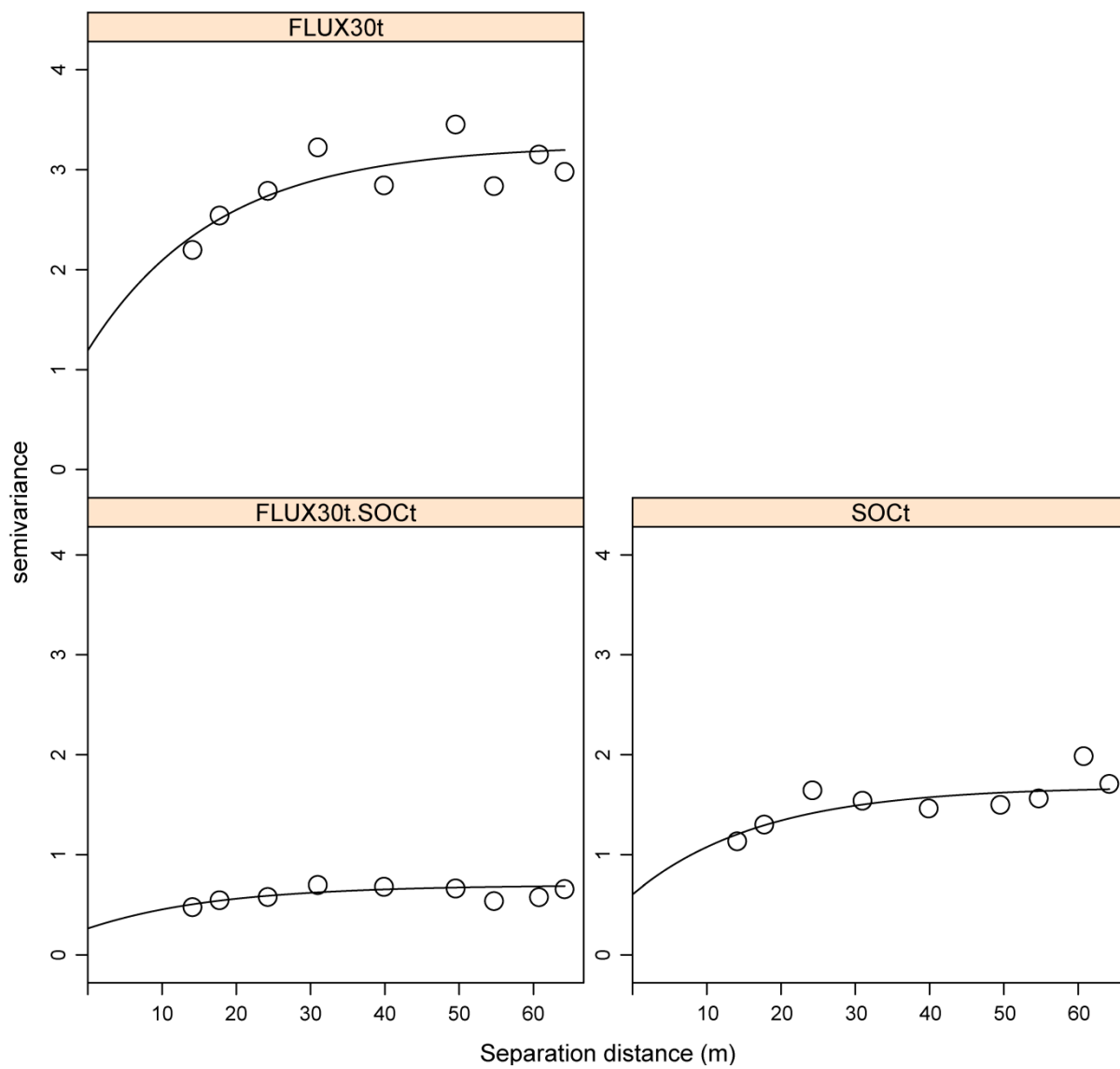
683 Figure 5

684



685

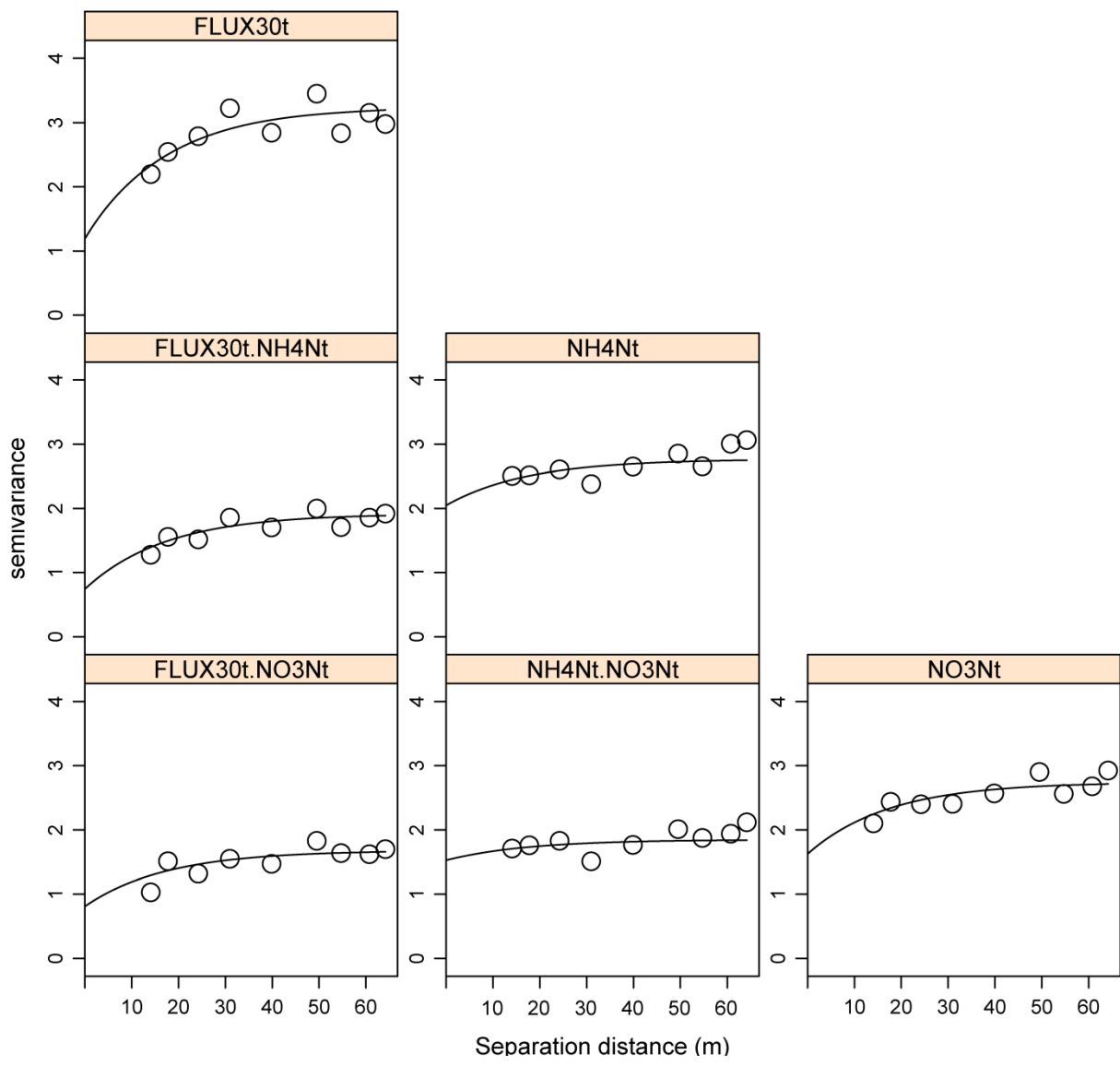
686 Figure 6



687

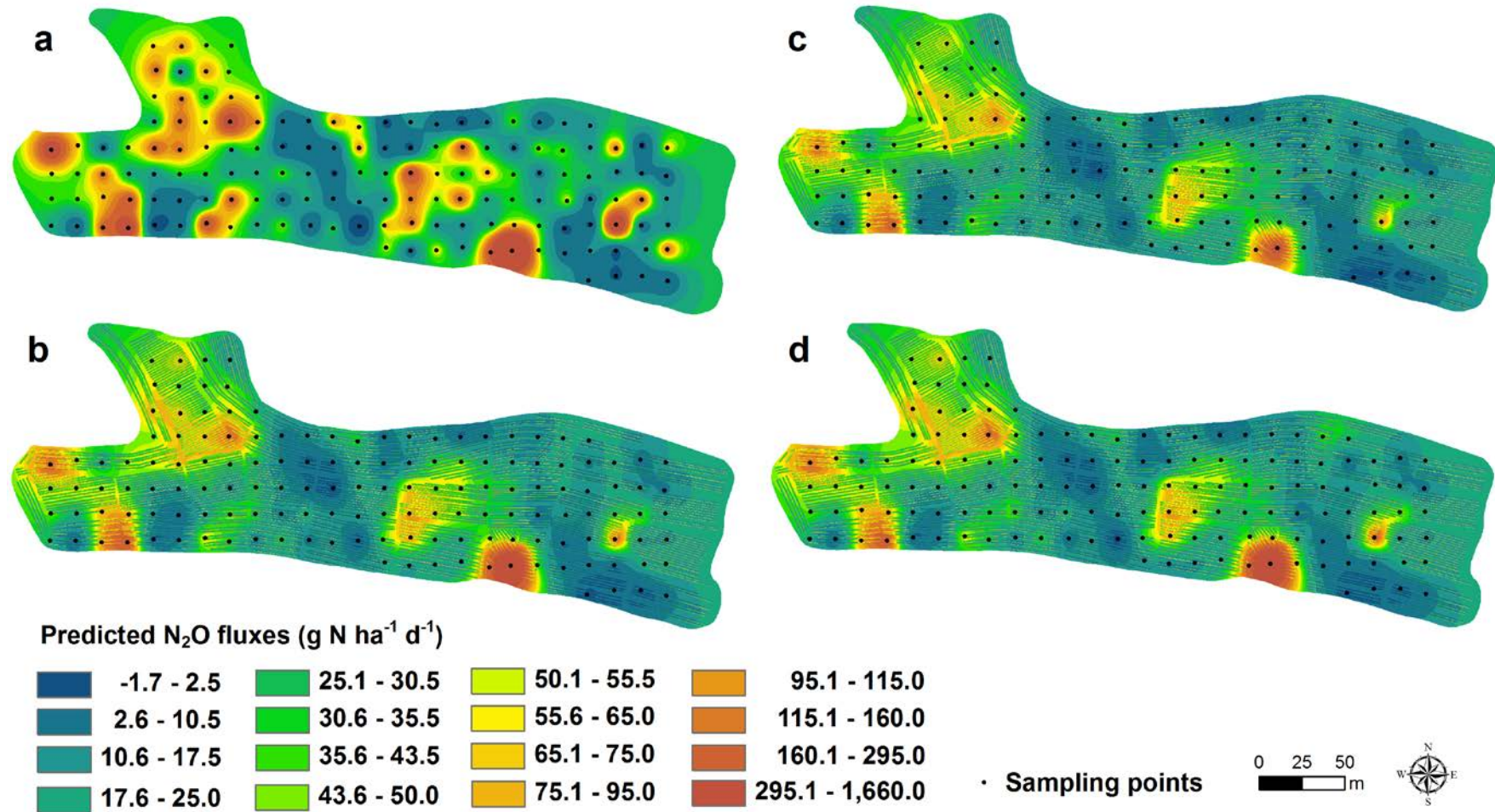
688 Figure 7

689

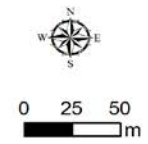
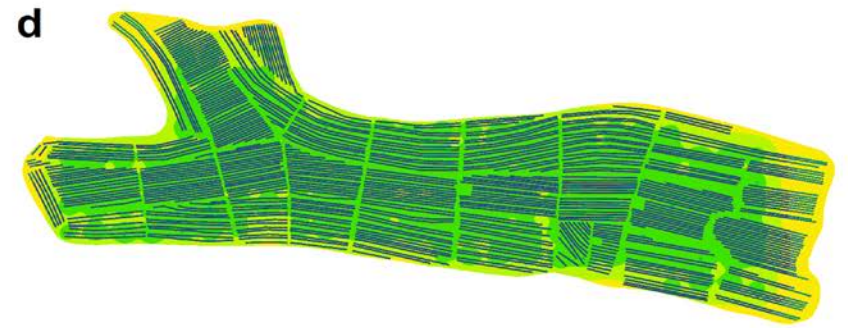
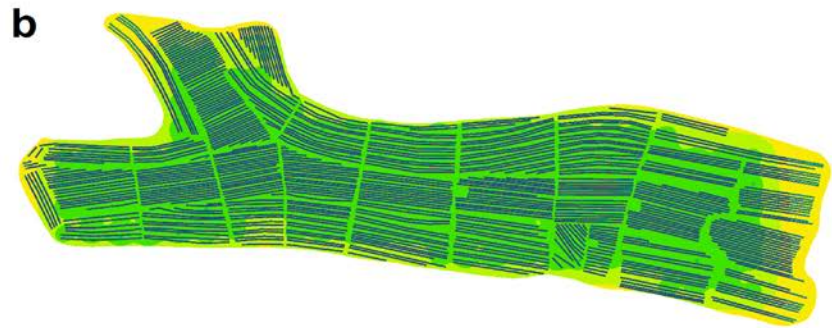
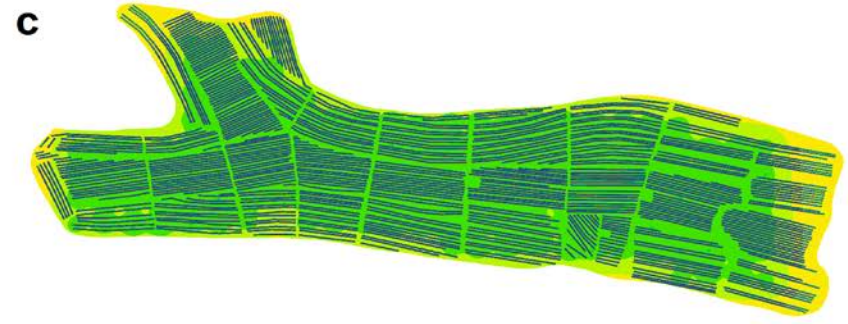
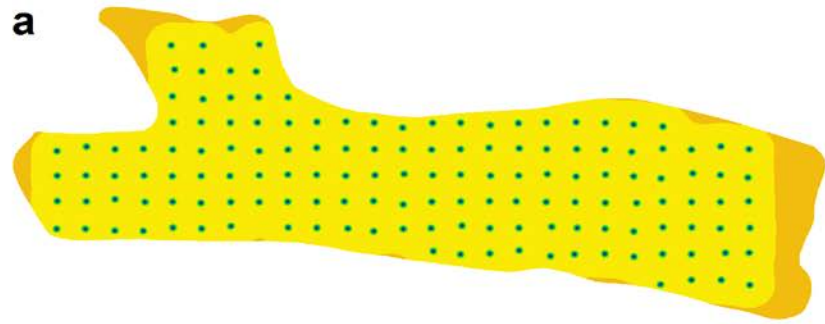


690

691 Figure 8



692
693 Figure 9
694



695
696
697
Figure 10